Spin–charge separation and topological phase transitions in Aharonov-Bohm rings of interacting electrons

Bruce Normand, K. Hallberg, A. A. Aligia, Arno P. Kampf

Angaben zur Veröffentlichung / Publication details:

Normand, Bruce, K. Hallberg, A. A. Aligia, and Arno P. Kampf. 2006. “Spin–charge separation and topological phase transitions in Aharonov-Bohm rings of interacting electrons.” *International Journal of Modern Physics B* 20 (19): 2651–55. https://doi.org/10.1142/s0217979206035138.

SPIN–CHARGE SEPARATION AND TOPOLOGICAL PHASE TRANSITIONS IN AHARONOV–BOHM RINGS OF INTERACTING ELECTRONS

B. NORMAND

Département de Physique, Université de Fribourg, CH-1700 Fribourg, Switzerland
bruce.normand@unifr.ch

K. HALLBERG

Centro Atómico Bariloche and Instituto Balseiro, Comisión Nacional de Energía Atómica, 8400 Bariloche, Argentina

A. A. ALIGIA

Centro Atómico Bariloche and Instituto Balseiro, Comisión Nacional de Energía Atómica, 8400 Bariloche, Argentina

A. P. KAMPF

Institut für Physik, Theoretische Physik III, Elektronische Korrelationen und Magnetismus, Universität Augsburg, 86135 Augsburg, Germany

We investigate the properties of strongly correlated electronic models on a flux-threaded ring connected to semi-infinite free-electron leads. The interference pattern of such an Aharonov-Bohm ring shows sharp dips at certain flux values, determined by the filling, which are a consequence of spin-charge separation in a nanoscopic system. The conductance through such a molecule or nanodevice is related directly to its spectroscopic properties, opening new experimental possibilities for probing the phenomenology of strongly interacting systems. As a further example, for a ring described by the half-filled ionic Hubbard model we show that the weight of the first conductance peak as a function of gate voltage or external flux allows one to identify the topological charge transition between a correlated insulator and a band insulator.

Keywords: Aharonov-Bohm ring; spin–charge separation; topological phase transition.

1. Introduction: Aharonov–Bohm Ring Geometry

Modern fabrication technology is essentially capable of preparing nanostructures to order, and of contacting and measuring systems of sizes down to the molecular scale. Recent investigations of nanoscopic structures have included quantum dot arrays, quantum dot chains, quantum dot molecules, mesoscopic rings, single molecules, nanocrystals and nanotubes. Here we consider the detection of certain phenomena which arise purely due to many–body correlation effects in such systems.

Strong electronic correlations invalidate the conventional quasiparticle description of Fermi liquids, and in one dimension (1D) lead to a "fractionalisation" of electronic excitations into separate spin and charge modes.[1] Spin–charge separation (SCS) has been sought experimentally in a variety of materials[2] and studied numerically in small systems.[3,4] The concept of the topological phase transition, in this case from a band insulator to a correlated insulator, is illustrated by a class of 1D systems described by the ionic Hubbard model (IHM),[5] and is relevant in a number of organometallic compounds.

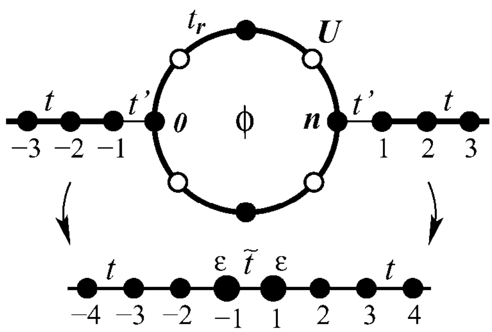

Fig. 1. Schematic representation of an interacting system on a ring connected by links t' to free-electron leads and threaded by a magnetic flux ϕ.

We study these phenomena by considering the transmittance of a flux–threaded, or Aharonov–Bohm (AB), ring (Fig. 1) of strongly interacting electrons attached to free–electron leads. This geometry was used to investigate the consequences of SCS in a Luttinger liquid.[4] The system can be considered as a chain containing two impurities (sites -1 and 1 in Fig. 1), and for small t' the transmittance is given by

$$T(\omega, V_g) = \frac{4\Gamma^2(\omega)|t_{\text{eff}}|^2}{|(\frac{\omega}{m} - \Delta\epsilon_{-1} + i\Gamma(\omega))(\frac{\omega}{m} - \Delta\epsilon_1 + i\Gamma(\omega)) - |t_{\text{eff}}|^2|^2}, \tag{1}$$

where the quantities

$$\Delta\epsilon_{-1}(\omega) = t'^2 g_{00}(\omega), \quad \Delta\epsilon_1(\omega) = t'^2 g_{nn}(\omega), \quad t_{\text{eff}}(\omega) = t'^2 g_{n0}(\omega) \tag{2}$$

depend only on the Green functions of the isolated ring. The line broadening Γ depends on the hybridisation with the leads and on their density of states, which also determines the integer $m = 1, 2$. The energy of the incoming electron is ω, and V_g is a gate voltage which may be used to control the relative energy of the ring and leads. This result is valid for systems with no spin degeneracy in the ground state.

2. Spin–Charge Separation

We consider the manifestations of SCS in an AB ring by using the t–J model as a canonical example of a strongly correlated system. The results for the transmission of the ring integrated over an energy window near the Fermi energy are shown in Fig. 2. The dips at specific flux values, $\phi_d \approx \pi(1 - 2n_s/N)$ for N electrons in the intermediate state, are a clear signature of SCS. These dips arise from destructive interference processes between specific pairs of states close to the Fermi energy, which then do not contribute to transport. Their dependence on the flux may be deduced by considering the $J \rightarrow 0$ limit, where the model is equivalent to the infinite–U Hubbard model and has SCS on all energy scales. Here the factorisation of the wavefunction[6,7] results in the spin part becoming equivalent only to an effective applied flux, which determines the values ϕ_d of the external flux responsible for destructive interference.[8] This nanoscopic SCS is robust for all values of the integration window, but breaks down when J is increased beyond the value t_r/L at which the spin subbands of different charge excitations become mixed. For odd N, at the flux values ϕ_d one may deduce effective spin and charge velocities which obey the relation $v_s/v_c = 1/N$.

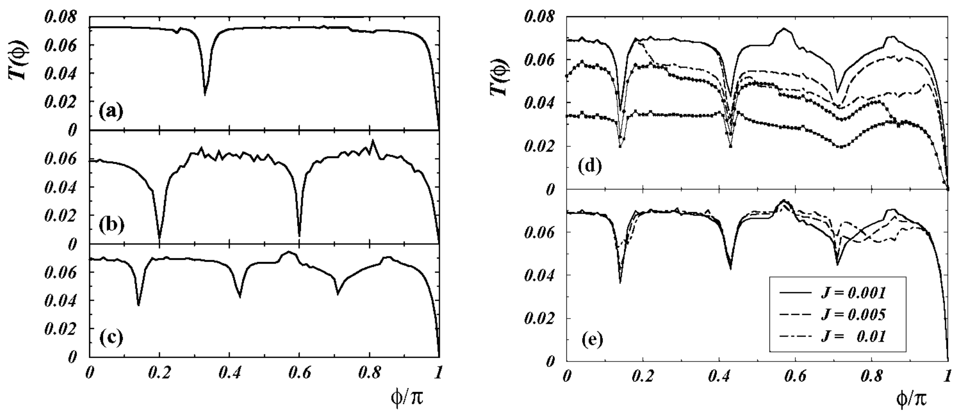

Fig. 2. $T(\phi)$ for one hole injected in an 8–site t_r–J ring with $J = 0.001t_r$, $t_r = t$ and $t' = 0.3t$. Dependence on particle number: (a) $N + 1 = 4$, (b) $N + 1 = 6$, (c) $N + 1 = 8$; (d) window size and (e) J.

3. Topological Phase Transitions

To illustrate the topological charge transition we consider an IHM with $U \sim 4t$ on the AB ring. The clear disappearance at $\phi = 0$ of the integrated peak weight for $U < U_c$ [Fig. 3(a)] marks the transition between the band and correlated insulator phases, which have different ground–state parities. This transition is topological in the sense that it is detected by a topological quantum number (the charge Berry phase) whose value changes by a discrete amount even in a finite system.

For a system with no ground–state degeneracy the properties of the spectral

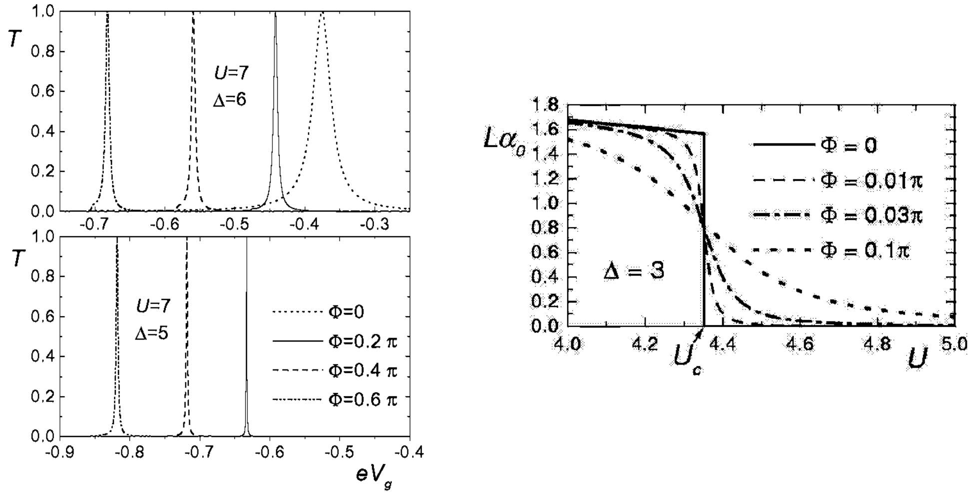

(a) (b)

Fig. 3. (a) $T(V_g)$ for V_g near the first peak in an 8–site IHM ring with leads at sites 0 and 2, $t_R = 1$, $t' = 0.2$, $\Delta = -3$ and U both below and above $U_c(L = 8) = 4.352$. (b) α_0 as a function of U for different values of flux ϕ.

peaks in Fig. 3(a) may be deduced from their lineshapes

$$T(z) \cong \frac{1}{1 + (z/w)^2} \frac{4\alpha_0 \alpha_n}{(\alpha_0 + \alpha_n)^2} + O((t'/\Gamma(0))^2), \tag{3}$$

where the quantities

$$\alpha_j = |\langle g(N-1)|c_{j\sigma}|g(N)\rangle|^2 \tag{4}$$

are analgous to spectral weights for local photoemission processes. The peak widths and integrated weights depend directly on α_0, which is difficult to measure in spectroscopic experiments, but can be obtained to high resolution by transport measurements. α_0 may then be used as the order parameter for the topological transition, which occurs for all values of t: in the band insulator it increases for decreasing ϕ, whereas in the correlated insulator $\alpha_0 \to 0$ as $\phi \to 0$. At $\phi = 0$, α_0 vanishes discontinuously at U_c [Fig. 3(b)], while the transition is smoother at finite flux (parity–breaking). For a system with a spin–degenerate ground state a Kondo resonance arises, which causes spectral peaks to become plateaux. This situation, which we investigate elsewhere,[9,10] is suppressed by finite temperatures or strong magnetic fields applied transverse to the ring.

4. Summary

We have demonstrated how the AB ring may be used as a probe for nanoscopic SCS and topological phase transitions. The ring transmittance is determined by interference effects, and allows access to the spectroscopic properties of the system. The signature of SCS is a sensitive dependence of integrated transmission on flux and doping, while the topological transition is the consequence of a change of ground–state symmetry. Experimentally, one may expect to detect these effects in quantum–dot rings if these could be fabricated with sufficiently high symmetry. Annular molecules may also offer a means of detecting the charge transition, which occurs as $\phi \to 0$, but nanoscopic SCS, which requires a threading flux on the order of a single flux quantum, appears beyond reach in single molecules. We comment that if a charged wire can be made to thread the ring, which may be realised with nested nanotubes, the possibility exists of detecting also an Aharonov–Casher effect.[11]

References

1. H. J. Schulz, *Int. J. Mod. Phys.* **B5**, 57 (1991).
2. C. Kim *et al.*, *Phys. Rev. Lett.* **77**, 4054 (1996).
3. E. A. Jagla, K. Hallberg, and C. A. Balseiro, *Phys. Rev.* **B47**, 5849 (1993).
4. E. A. Jagla and C. A. Balseiro, *Phys. Rev. Lett.* **70**, 639 (1993).
5. S. R. Manmana, V. Meden, R. M. Noack and K. Schoenhammer, *Phys. Rev.* **B70**, 155115 (2004).
6. M. Ogata and H. Shiba, *Phys. Rev.* **B41**, 2326 (1990).
7. A. Schadschneider, *Phys. Rev.* **B51**, 10386 (1995).
8. K. Hallberg, A. A. Aligia, A. P. Kampf and B. Normand, *Phys. Rev. Lett.* **93**, 067203 (2004).
9. A. A. Aligia, K. Hallberg, B. Normand and A. P. Kampf, *Phys. Rev. Lett.* **93**, 076801 (2004).
10. A. A. Aligia and L. A. Salguero, *Phys. Rev.* **B70**, 075307 (2004).
11. A. Balatsky and B. Altshuler, *Phys. Rev. Lett.* **70**, 1678 (1993).